Enhanced Hot-Carrier Cooling and Ultrafast Spectral Diffusion in Strongly Coupled PbSe Quantum-Dot Solids

ARTICLE *in* NANO LETTERS · DECEMBER 2011

Impact Factor: 13.59 · DOI: 10.1021/nl203235u · Source: PubMed

7 AUTHORS, INCLUDING:

Michiel Aerts
Delft University of Technology
10 PUBLICATIONS **171** CITATIONS
SEE PROFILE

Juleon M Schins
Delft University of Technology
79 PUBLICATIONS **2,560** CITATIONS
SEE PROFILE

Arjan J Houtepen
Delft University of Technology
68 PUBLICATIONS **1,473** CITATIONS
SEE PROFILE

Laurens D A Siebbeles
Delft University of Technology
249 PUBLICATIONS **7,274** CITATIONS
SEE PROFILE

NANO LETTERS

LETTER

pubs.acs.org/NanoLett

Enhanced Hot-Carrier Cooling and Ultrafast Spectral Diffusion in Strongly Coupled PbSe Quantum-Dot Solids

Yunan Gao,[†,‡] Elise Talgorn,[†] Michiel Aerts,[†] M. Tuan Trinh,[†,§] Juleon M. Schins,[†] Arjan J. Houtepen,[*,†] and Laurens D. A. Siebbeles[†]

[†]Optoelectronic Material Section, Department of Chemical Engineering, Delft University of Technology, Julianalaan 136, 2628 BL, Delft, The Netherlands

[‡]The Kavli Institute of Nanoscience, Delft University of Technology, Lorentzweg 1, 2628 CJ, Delft, The Netherlands

Supporting Information

ABSTRACT: PbSe quantum-dot solids are of great interest for low cost and efficient photodetectors and solar cells. We have prepared PbSe quantum-dot solids with high charge carrier mobilities using layer-by-layer dip-coating with 1,2-ethanediamine as substitute capping ligands. Here we present a time and energy resolved transient absorption spectroscopy study on the kinetics of photogenerated charge carriers, focusing on 0−5 ps after photoexcitation. We compare the observed carrier kinetics to those for quantum dots in dispersion and show that the intraband carrier cooling is significantly faster in quantum-dot solids. In addition we find that carriers diffuse from higher to lower energy sites in the quantum-dot solid within several picoseconds.

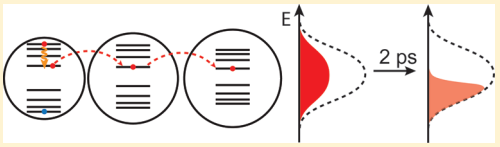

KEYWORDS: Quantum dots, photoconductivity, carrier dynamics, carrier cooling, optoelectronic materials, photovoltaics

Films of colloidal quantum dots (QDs), often called QD solids, have recently experienced a significant increase in attention. This was triggered by the successful preparation of photodetectors,[1] field-effect transistors,[2] and solar cells[3−9] of such films. In these devices the QDs are electronically coupled by removing or replacing the original bulky surfactants. The resulting smaller interparticle distances result in overlapping wave functions and a significant increase in the mobility of charge carriers, to an extent at which they become sufficient for device applications. This wave function overlap is especially large in films of Pb chalcogenide QDs owing to the small effective masses of electrons and holes in these materials. The fact that PbS and PbSe QD solids can be used to prepare solar cells with promising efficiencies implies that photoexcitation of the QDs results in mobile charge carriers that are able to reach the electrodes of the device. However, very little information is available about the rate and mechanism of mobile charge carrier photogeneration and the carrier kinetics on an ultrafast time scale. Information on these topics serves to guide the enhancement of the performance of QD optoelectronic devices.

Here we present a study of ultrafast electron and hole dynamics in strongly coupled PbSe QD solids, focusing on the first few picoseconds after excitation. We distinguish two separate relaxation processes that occur on this time scale: hot carrier relaxation from higher levels to the 1S electron and hole levels (intraband carrier cooling) and carrier relaxation due to hopping between different QDs (referred to as spectral diffusion). We show that intraband carrier cooling is significantly enhanced in these QD solids with respect to QDs in dispersion: the cooling rate is $(0.25 \pm 0.01\ \text{ps})^{-1}$ vs $(0.69 \pm 0.01\ \text{ps})^{-1}$ in dispersion. This enhanced hot carrier cooling rate in strongly coupled QD solids could be an issue of concern for the development of hot carrier QD solar cells. In addition, by performing spectrally resolved transient absorption spectroscopy (TA), we demonstrate that the excited charge carriers undergo rapid spectral diffusion by hopping to lower energy sites in the ensemble of (1S) states of the QD solid. This spectral diffusion is complete in 2 ps. Spectral diffusion via energy transfer of excitons has been reported for PbS QD solids with a transfer time of 200−400 ns,[10] and it has been suggested that exciton energy transfer in fully optimized CdSe quantum dot systems could be as fast as 40 ps.[11] The spectral diffusion reported here results from the movement of free charge carriers, rather than excitons, and is significantly faster. This is in line with the very high carrier mobilities of 3 $\text{cm}^2/(\text{V s})$ that we determine for this sample, using the time-resolved microwave conductivity (TRMC) technique. The picosecond spectral diffusion presents a direct and very clear visualization of the high hopping rates in this system.

PbSe QDs were synthesized following ref 12 and used to prepare QD films with a layer-by-layer (LBL) procedure, using 1,2-ethanediamine (EDA) as capping ligands to substitute for the much longer original oleylamine ligands. Full details on the synthesis and film preparation can be found in the Supporting Information. Figure 1a shows a high-resolution TEM image of a reference sample prepared on SiN TEM grids. This image shows that the QDs do not fuse together into large clusters or wires. Close inspection of Figure 1a shows clearly that the lattice planes of different QDs are different. If the QDs would sinter, they would

Received: September 16, 2011
Revised: October 26, 2011
Published: October 31, 2011

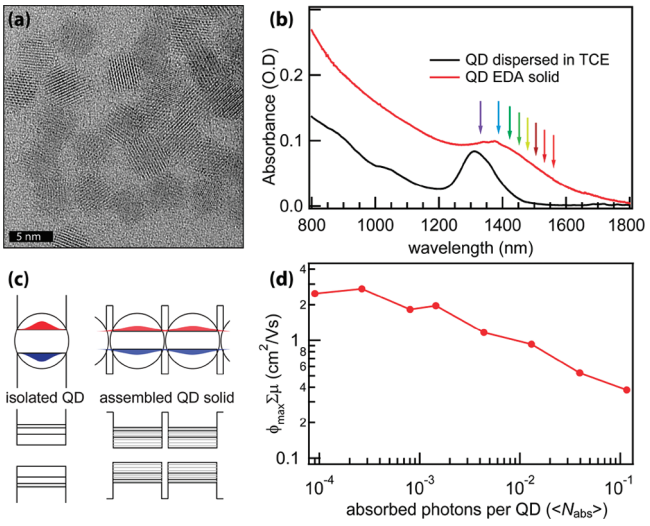

Figure 1. (a) High-resolution TEM image of a PbSe QD film grown using the layer-by-layer technique. (b) Absorption spectra of a QD colloidal dispersion and a QD solid. The colored arrows indicate the probe wavelengths used in the experiments described in the text. (c) Schematic of electronic coupling in PbSe QD solids. Overlapping wave functions result in the formation of electronic minibands. (d) The product $\phi_{max}\Sigma\mu$ of the charge carrier generation yield and the sum of electron and hole mobilities obtained from time-resolved microwave conductivity measurements, as a function of the number of absorbed photons per QD.

have a strong tendency to align their lattice planes, as this lowers the total free energy of the crystal.[13] This shows that no significant sintering has occurred during the layer-by-layer deposition process. The QDs in the films do not form an ordered superlattice and have a very short interparticle separation in line with the 0.38 nm length of the 1,2-ethanediamine linker molecules.

Optical absorption spectra of QDs dispersed in tetrachloroethylene (TCE) and deposited in QD solids are shown in Figure 1b. The spectrum of the QD solids shows significant broadening with respect to the spectrum of the dispersion, but clearly still exhibits quantum confinement. Such a broadening could be due to increased polydispersity, disorder in dielectric environment resulting in a spatial variation of polarization energies, or strong electronic coupling as shown schematically in Figure 1c.

We have used the TRMC technique[14,15] to determine the photoconductivity and the carrier mobility of these samples. This technique involves 3 ns pulsed laser excitation in combination with time-resolved microwave absorption measurements to determine the product $\phi_{max}\Sigma\mu$ of the yield of charge carrier generation ϕ_{max} (i.e., the number of free electrons and holes per absorbed photon at the maximum of the transient microwave photoconductivity) and the sum $\Sigma\mu$ of the electron and hole mobility. Experimental details are available in the Supporting Information. Figure 1d shows $\phi_{max}\Sigma\mu$ as a function of the average number $\langle N_{abs}\rangle$ of photons absorbed per QD. $\langle N_{abs}\rangle$ is obtained as $I_0\sigma$, where I_0 is the fluence of the excitation pulse and σ is the absorption cross section taken from ref 16. At excitation densities above $\sim 10^{-3}$ absorbed photons per QD the observed $\phi_{max}\Sigma\mu$ value decreases with increasing laser fluence, due to higher order charge recombination during the 3 ns laser pulse. At the lowest excitation densities the product $\phi_{max}\Sigma\mu$ is independent of the number of absorbed photons per QD. This shows that higher order recombination of charge carriers is absent at low excitation density. The value of the product $\phi_{max}\Sigma\mu$ is 3 cm^2/(V s). We have shown recently that for the strongly coupled PbSe QD solids investigated here, photoexcitation results in mobile charge carriers with unity efficiency[17] and with a decay time of $\sim$10 ns. This implies that $\phi_{max} \approx 1$ and the sum of the electron and hole mobility is several cm^2/(V s).

Electronic coupling between quantum dots can result in a broadening of the optical absorption spectrum, as observed in Figure 1b. For a two states system with identical energy, the coupling energy is $\beta = h\Gamma/4$ where h is the Planck constant and Γ the tunnel rate.[18] The tunnel rate can be estimated from the mobility μ using the Einstein−Smoluchowski relation: $\Gamma = \mu k_B T/(ea^2)$, where e is the elementary charge, a is the hopping distance (the center-to-center distance), k_B is Boltzmann's constant, and T is the temperature. Using a hopping distance of 4.2 nm and a mobility of 3 cm^2/(V s) yields a tunnel rate of $\Gamma = (2\ \text{ps})^{-1}$ at room temperature. Note that this is the rate with which a charge carrier hops to a specific neighbor site.[19] The total rate of hopping out of a specific quantum dot is $\Gamma_{tot} = z\Gamma = (0.17\ \text{ps})^{-1}$, assuming the number z of nearest neighbors is 12 (as in a closed packed lattice). For square/cubic lattices and considering only nearest-neighbor interaction between states with identical energy, the tight-binding approximation predicts a simple relationship between bandwidth W, number of nearest neighbors z, and nearest-neighbor coupling energy β: $W = 2z\beta$.[20] While the QDs do not organize in a cubic lattice (see Figure 1a), we can still use this equation to make a rough estimate of the broadening that is expected for a given coupling energy. This yields a bandwidth of 11 meV, while the full width at half-maximum (fwhm) of the 1S absorption peak increases from 110 meV in dispersion to 220 meV in the QD solids.

It appears that the measured mobility is not high enough to explain the observed broadening of the optical absorption. One could imagine that the carrier mobility is limited by domain boundaries, while the optical broadening is determined by local strong coupling. With a total hopping rate of $\Gamma_{tot} = (0.17\ \text{ps})^{-1}$ the charge carriers undergo $\sim$350 hops within half a period of the 8.4 GHz microwave field (which amounts to 60 ps). The volume probed by a charge thus contains hundreds of QDs, and it is likely that within that volume several QDs are only weakly coupled, limiting the measured carrier mobility. The optical broadening is determined by coupling on a more local scale. In the tight-binding approximation for a one-dimensional system, the coupling between two levels produces already half the bandwidth of an infinite number of coupled levels.[21] However, we have recently prepared PbSe QD solids with similar mobilities, and much more narrow absorption spectra, using Br^- atomic ligands.[22] In addition an electron mobility of 16 cm^2/(V s) has recently been reported for a QD solid prepared from CdSe QDs with inorganic $In_2Se_3^{2-}$ ligands.[23] In this system quantum confinement was still clearly observable in the optical absorption. This suggests that the absorption broadening we observe is not fully determined by electronic coupling.

To investigate the ultrafast carrier kinetics, we have applied transient absorption spectroscopy. The samples are excited by a 795 nm laser pulse, well above the band edge of $\sim$1320 nm, with an excitation density of several photons per hundred QDs. The 1S carrier occupation was monitored selectively by probing the $1S_h1S_e$ transition bleach (Figure 1b). Experimental details are available in the Supporting Information. The absorption bleach of the $1S_h1S_e$ transition (i.e., $\Delta T/T > 0$) is linearly proportional to the carrier occupation in the $1S_e$ and $1S_h$ levels.[24−26] However,

dx.doi.org/10.1021/nl203235u |Nano Lett. 2011, 11, 5471–5476

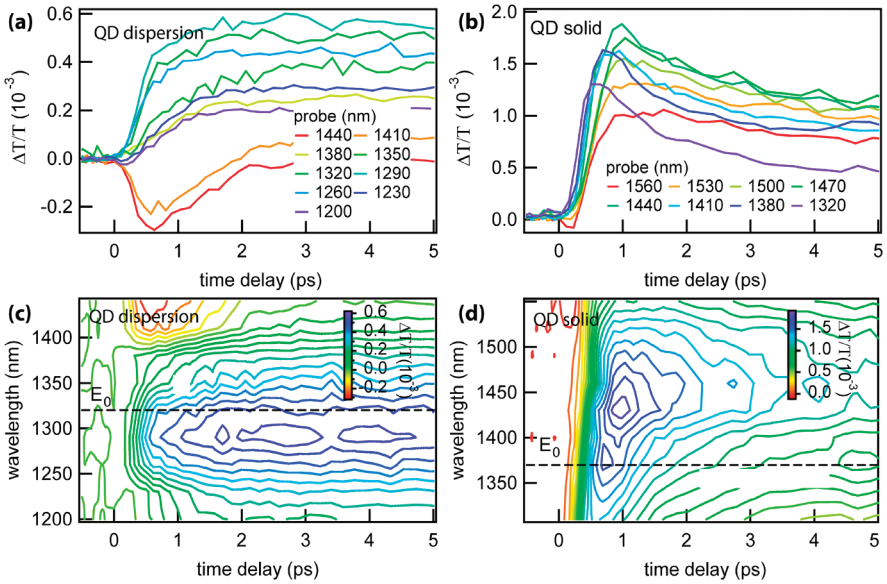

Figure 2. Transient absorption spectra at low pump intensity and various probe wavelengths near the $1S_h1S_e$ transition: (a) for a QD dispersion ($\langle N_{abs}\rangle$ = 0.04) and (b) for a QD solid ($\langle N_{abs}\rangle$ = 0.03). Also shown are contour plots of the same data for the QD dispersion (c) and the QD solid (d), illustrating that the position of wavelength at maximum bleach is essentially constant for the dispersion, while a clear red shift of the maximum bleach position is observed for the QD solid. The dashed lines in (c) and (d) denote the ground state absorption maximum.

as shown below, the wavelength of maximum optical absorption may shift significantly as a function of time. This implies that a detailed analysis of carrier dynamics requires spectrally resolved measurements.

Figure 2 presents selected absorption transients for a PbSe QD dispersion (a and c) and a QD solid (b and d) at a pump wavelength of 795 nm and several probe wavelengths in the $1S_h1S_e$ transition profile, corresponding to the solid arrows in Figure 1b. The probe wavelength dependence of the absorption transients for QD dispersions has been studied by Ellingson et al.[27] and Trinh et al.[26,28] In QD dispersions two effects, state filling (absorption bleach) and Coulomb interactions between multiple excitons (absorption shift), determine the transient absorption features.

It is evident from panels a and b of Figure 2 that both in dispersion and in the QD solid the absorption transients depend strongly on the probe wavelength. For QD dispersions this is due to a red shift of the optical transitions upon photoexcitation.[26,27] This so-called biexciton shift occurs both for hot carriers, directly after excitation, and for thermalized carriers. However it is typically larger in the former case.[26] Inspection of the contour plots in panels c and d of Figure 2 reveals remarkable differences between the QD dispersion and the QD solid: the wavelength of maximum absorption bleach changes much more drastically in the QD solid and the phenomenon continues for a significantly longer time. In the QD solid the wavelength of the bleach maximum is initially at the blue side of the ground state absorption maximum, but it shifts approximately 80 nm to the red and saturates after ~2 ps. For the QD dispersion the bleach maximum develops at the blue side of the absorption maximum and remains there. Clearly the carrier dynamics are very different in the two cases.

Analysis. To analyze the ultrafast carrier dynamics in detail and to be able to separate the effects of carrier decay and spectral changes we have used a fitting procedure on the spectrally resolved transient absorption data. The absorption spectrum in the probed spectral region can be approximated by a single Gaussian function. The following function is used to describe the transient absorption data

$$\begin{aligned}\Delta A(E,t) \quad &= \\ \langle N_{abs}\rangle &\left(A(t)e^{-\{E-[E_0+\Delta E(t)]\}^2/2w^2} - A_0 e^{-(E-E_0)^2/2w^2}\right) \\ = \langle N_{abs}\rangle A_0 &\left(A_F(t)e^{-\{E-[E_0+\Delta E(t)]\}^2/2w^2} - e^{-(E-E_0)^2/2w^2}\right)\end{aligned} \quad (1)$$

The $\langle N_{abs}\rangle$ term accounts for the fact that only excited QDs show a change of the absorption. The first term between brackets represents the absorption profile of the $1S_h1S_e$ transition for excited QDs, and the second term represents the ground state absorption. The fit parameters A_0, E_0, and w are obtained from fitting the independently obtained steady state absorption spectrum, and $\langle N_{abs}\rangle$ is determined from the excitation fluence and the absorption cross section.[16] The amplitude $A(t)$ and the energy shift $\Delta E(t)$ of the excited state absorption are allowed to vary and are determined by fitting eq 1 to the transient absorption spectra of panels c and d of Figure 2. The resulting fractional amplitudes $A_F(t) = A(t)/A_0$ are displayed in Figure 3a; the energy shifts $\Delta E(t)$ are shown in Figure 3b.

Intraband Carrier Cooling. Excitation of the samples with 795 nm pump light results in the creation of hot carriers. Since the $1S_h1S_e$ transition is probed, an absorption bleach will only develop when the hot carriers have cooled down to the 1S levels. This is in contrast to biexciton shifts resulting from the presence of hot carriers. Figure 3a shows that for the QD dispersion the absorption amplitude decreases gradually during ~2 ps. This reveals the cooling process. In contrast the absorption amplitude for the QD solid changes much faster. The absorption amplitude reaches a minimum around 0.5 ps time delay and subsequently increases. This increase implies a charge carrier decay process. Figure 1d shows that at the used excitation density of 0.03 absorbed photons per QD, higher order decay processes are

dx.doi.org/10.1021/nl203235u |Nano Lett. 2011, 11, 5471–5476

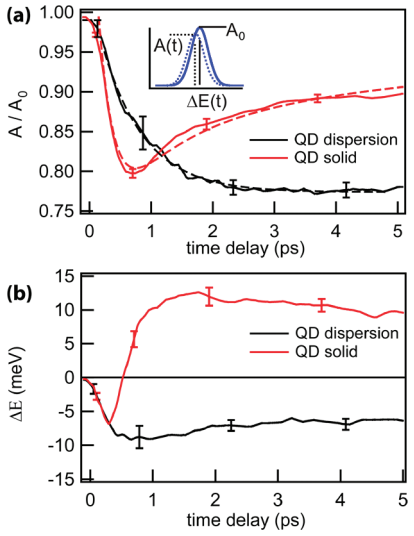

Figure 3. (a) Transients of the fractional absorption amplitude (obtained by fitting eq 1 to the transient absorption spectra in Figure 2) for a QD dispersion (black curves) and a QD solid (red curves). The solid lines represent extracted fractional amplitudes; the dashed lines result from fitting eqs 2−5 to the data. (b) The energy shift of the $1S_h1S_e$ absorption maximum for a QD dispersion (black curves) and a QD solid (red curves). Error bars indicate the standard deviation of the extracted bleach amplitudes and energy shifts.

important. This higher order carrier decay is attributed to diffusion mediated Auger recombination between two electrons and a hole, or between two holes and an electron.[14,15,29]

To quantify the carrier dynamics the following function has been fitted to the amplitudes in Figure 3a

$$A_F(t) = 1 - Cn_{1s} \quad (2)$$

This function describes that the bleach of the $1S_h1S_e$ transition is linear with the number of charges in the 1S electron and hole levels. n_{1s} represents the number of electrons and holes in the 1S levels, i.e., $n_{1s} = 1$ implies the presence of both an electron and a hole in these levels. The number of charge carriers in the 1S levels is obtained from the following coupled rate equations

$$\frac{dn_{hot}}{dt} = \frac{-n_{hot}}{\tau_{hot}} \quad (3)$$

$$\frac{dn_{1s}}{dt} = \frac{n_{hot}}{\tau_{hot}} \text{ (for QD dispersions)} \quad (4)$$

$$\frac{dn_{1s}}{dt} = \frac{n_{hot}}{\tau_{hot}} - k_3 n_{1s}^3 \text{ (for QD solids)} \quad (5)$$

n_{hot} is the number of hot charge carriers and τ_{hot} is the hot carrier lifetime. The absorption amplitude in Figure 3a is only determined by those QDs that are photoexcited, due to the $\langle N_{abs} \rangle$ term in eq 1. Since an excited QD contains one electron and one hole (carrier multiplication does not occur at this pump photon energy[30]), the initial value of n_{hot} is 1. The number of 1S charges grows as hot carriers cool down. At the same time decay channels may reduce the number of 1S carriers. For both the QD dispersions and QD solids, trapping processes and radiative recombination occur on a nanosecond to microsecond time scale,[29] so they can be ignored on the picosecond time scale considered here. For QD solids a third-order decay term, with rate constant k_3, is included in eq 5 to incorporate the effect of Auger recombination of charge carriers. This Auger recombination will be the topic of a forthcoming publication and is not discussed here. These equations are used to fit the solid curves in Figure 3a; the resulting fits are shown as the dashed lines in the same figure.

In the simplest model the presence of an electron and a hole in the 1S levels results in a fractional absorption bleach of 1/4.[28] Thus, the expected value for the fit parameter C in eq 2 is 0.75. From our fits we find that C is 0.78 for the QD dispersion and 0.77 for the QD solid, in line with the expected value. We find that the carrier cooling time τ_{hot} is 0.69 ± 0.01 ps for QDs in dispersion, in line with existing literature values.[31] For the QD solid we find a significantly faster cooling time of 0.25 ± 0.01 ps. We have calibrated our setup by using the same experimental settings to determine the response time for a single crystalline GaAs films and determined a 0.1 ps response time. This shows that the 0.25 ps cooling time obtained for the QD solid is not limited by the time resolution of the experiment.

The discrete nature of electronic states in colloidal QDs has been predicted to significantly slow down the cooling rate, relative to bulk materials, as a result of the so-called phonon bottleneck.[32,33] However hot carrier cooling in QDs turned out to be much faster than expected.[34,35] For PbSe QD dispersions Schaller et al. determined size-dependent 1P to 1S cooling times ranging from 2.5 ps (for the largest QDs) to 0.25 ps (for very small QDs).[31] The Guyot−Sionnest group has put forward a convincing explanation for the fast hot-carrier relaxation in QDs. They have shown that energy is transferred to ligand vibrational modes, during the cooling process.[36−38] These ligand vibrational modes have energies that can match the spacing of the QD energy levels, resulting in fast carrier relaxation.

When QDs are assembled into QD solids the original oleylamine ligands are replaced by 1,2-ethanediamine. This strongly reduces the number of CH groups (see FTIR spectra in the Supporting Information) while keeping the same ligand headgroup. Hence, little effect on the rate of energy transfer to ligand vibrations is expected, and if such an effect exists it would be to slow down energy transfer due to the smaller number of available CH vibrational modes. Instead we speculate that increased electronic coupling, as evidenced by the high charge carrier mobilities, results in the formation of a quasi-continuum of bandlike electronic states in the QD solid.[23,29] This band formation decreases the number of lattice phonons that need to be emitted in successive steps during phonon assisted thermalization and would thereby increase the cooling rate.

To test this hypothesis we have prepared QD solids with the longer substitute capping ligand 1,4-benzenediamine (BDA). The larger separation between QDs results in a 10-fold lower mobility and a concomitant smaller electronic coupling than for QD solids with EDA ligands (see Figure S2 in the Supporting Information). In the QD solids with BDA ligands we determine a cooling rate of $(0.40 \pm 0.01 \text{ ps})^{-1}$ (Figure S2c, Supporting Information), which is in between the cooling rates of the dispersion and the QD solid with EDA ligands. This shows that the extent of electronic coupling influences the intraband cooling rate, in line with our hypothesis.

The intraband cooling rate is an important parameter for several applications of quantum dots. For instance, in a hot carrier solar cell the excess energy above the band edge is used by extracting hot charges before they thermalize.[39] Quantum dots

dx.doi.org/10.1021/nl203235u |Nano Lett. 2011, 11, 5471–5476

are considered as suitable materials for hot carrier solar cells, because the hot carrier cooling rates may be lower than in bulk semiconductors.[40] The enhanced hot carrier cooling rate in strongly coupled QD solids could be an issue of concern for the development of hot carrier QD solar cells.

Spectral Diffusion. Figure 3b displays the time-dependent energy shift of the 1S absorption maximum for QDs in dispersion (black line) and for the QD solid (red line). The shifts are obtained by fitting eq 1 to the contour plots in panels c and d of Figure 2. The quantum dot dispersion shows a fast red shift of ~8 meV that develops in less than 0.5 ps, decreases slightly during 3 ps, and subsequently becomes constant. This behavior can be understood as the quick generation of hot charge carriers during the laser pulse, resulting in a repulsive biexciton interaction between the exciton generated by the pump pulse and the exciton generated by the probe pulse. As shown above these hot charge carriers cool down during ~2 ps (τ_{hot} = 0.7 ps). In line with previous observations by Trinh et al.[26] and Ellingson et al.[27] the biexciton shift decreases slightly as carriers cool down to the 1S levels, after which it becomes constant.

The QD solid also shows an initial red shift of a magnitude that is comparable to the red shift of the QD dispersion (red line in Figure 3b). Apparently, the biexciton shift is similar in film and dispersion. After ~0.5 ps the red shift starts to decrease and develops into a blue shift of ~12 meV during 2 ps. Since intraband carrier cooling in the film is much faster, this developing blue shift cannot be related to cooling of carriers from higher levels to the 1S electron and hole levels. In addition, intraband carrier cooling might reduce the observed red shift, but it is not expected to result in a blue shift.

As shown by the TRMC measurements in Figure 1d, carriers in these films are highly mobile. Hopping from higher to lower energy sites occurs with a higher hopping rate than the reverse. As a result of the difference in hopping rates, the carrier occupation shifts from an initially flat distribution function (determined by the absorption probability of the QDs) to a Fermi−Dirac distribution. This is shown schematically in Figure 4a. Hence, electrons and holes will gradually start occupying lower energy sites in the ensemble, resulting in a bleach at the red side of the absorption peak and a blue shift of the absorption maximum. Therefore, the observed blue shift can be attributed to spectral diffusion caused by interparticle thermalization of charge carriers.

After ~2 ps the blue shift becomes constant, indicating the charge carriers have reached thermal equilibrium. This picosecond spectral diffusion may be understood by considering the hopping rate of charge carriers. As mentioned earlier, the charge carrier mobility of 3 $cm^2/(V\ s)$ measured by TRMC can be related via the Einstein−Smoluchowski relation to a total hopping rate of $\Gamma_{tot} = (0.17\ ps)^{-1}$. It should be pointed out that the mobility determined by TRMC is the average mobility after several nanoseconds, i.e., after thermalization. We have used the Miller−Abrahams hopping model to estimate the average hopping rate before and after thermalization. Details are included in the Supporting Information and the results are shown in Figure 4b. The mobility of charge carriers is significantly higher before thermalization. The extent of this effect depends on the number of charge carriers per QD. For the carrier density of $\langle N_{abs} \rangle = 0.03$, used in our experiments, the average hopping rate is ~10 times higher before thermalization. Considering this effect the average hopping rate could be as high as $\sim(0.017\ ps)^{-1}$, which means that carriers undergo more than 100 hops within 2 ps. This number of hopping steps appears to be sufficient to establish thermal equilibrium.

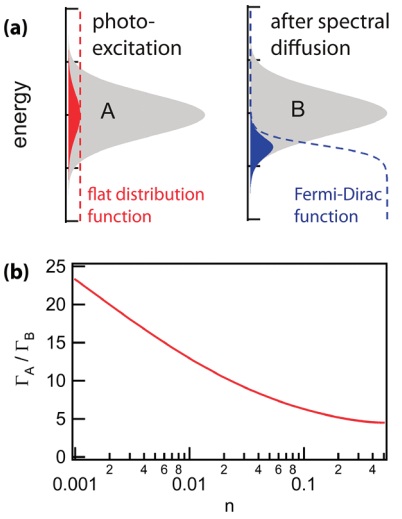

Figure 4. (a) A schematic of the density of 1S states in the QD solid (gray area) and a distribution function that is flat (red dashed line) directly after photoexcitation (situation A), turning into a Fermi−Dirac function (blue dotted line) after spectral diffusion (situation B). The red and blue areas show the charge carrier distributions before and after thermalization, respectively. (b) The ratio between the hopping rate before and after thermalization as a function of charge density n (number of electrons per QD) obtained by a numerical calculation using the Miller−Abrahams model.

In conclusion, we have observed that in QD solids hot carrier cooling becomes faster with increased electronic coupling and is significantly enhanced compared to the cooling rate for QDs in dispersion. This suggests that strong electronic coupling is an issue of concern for hot carrier QD solar cells. In addition we observe fast spectral diffusion indicative of efficient interparticle thermalization in ~2 ps. The picosecond spectral diffusion presents a direct visualization of the high hopping rates in this system.

■ ASSOCIATED CONTENT

Supporting Information. Details concerning the sample preparation and the characterization methods, infrared absorption spectra, and additional results on QD solids with 1,4-benzenediamine ligands. This material is available free of charge via the Internet at http://pubs.acs.org.

■ AUTHOR INFORMATION

Corresponding Author

*E-mail: A.J.Houtepen@tudelft.nl.

Present Addresses

§van der Waals—Zeeman Institute, University of Amsterdam, Science Park 904, 1098 XH Amsterdam, The Netherlands.

■ ACKNOWLEDGMENT

This work has been financially supported by the 3TU Centre for Sustainable Energy Technologies (Federation of the Three Universities of Technology in The Netherlands). E.T. acknowledges support by SenterNovem (project SELECT). M.A. acknowledges financial support by the Advanced Dutch Energy

Materials program of the Dutch Ministry of Economic Affairs, Agriculture and Innovation. A.J.H. acknowledges financial support by The Netherlands Organisation for Scientific Research (NWO) through a NWO-VENI grant.

REFERENCES

(1) Konstantatos, G.; Howard, I.; Fischer, A.; Hoogland, S.; Clifford, J.; Klem, E.; Levina, L.; Sargent, E. H. *Nature* **2006**, *442* (7099), 180–183.
(2) Talapin, D. V.; Murray, C. B. *Science* **2005**, *310* (5745), 86–89.
(3) Leschkies, K. S.; Beatty, T. J.; Kang, M. S.; Norris, D. J.; Aydil, E. S. *ACS Nano* **2009**, *3* (11), 3638–3648.
(4) Choi, J. J.; Lim, Y. F.; Santiago-Berrios, M. B.; Oh, M.; Hyun, B. R.; Sung, L. F.; Bartnik, A. C.; Goedhart, A.; Malliaras, G. G.; Abruna, H. D.; Wise, F. W.; Hanrath, T. *Nano Lett.* **2009**, *9* (11), 3749–3755.
(5) Gur, I.; Fromer, N. A.; Geier, M. L.; Alivisatos, A. P. *Science* **2005**, *310* (5747), 462–465.
(6) Kim, S. J.; Kim, W. J.; Cartwright, A. N.; Prasad, P. N. *Appl. Phys. Lett.* **2008**, *92* (19), 191107.
(7) Luther, J. M.; Law, M.; Beard, M. C.; Song, Q.; Reese, M. O.; Ellingson, R. J.; Nozik, A. J. *Nano Lett.* **2008**, *8* (10), 3488–3492.
(8) Ma, W.; Luther, J. M.; Zheng, H. M.; Wu, Y.; Alivisatos, A. P. *Nano Lett.* **2009**, *9* (4), 1699–1703.
(9) Pattantyus-Abraham, A. G.; Kramer, I. J.; Barkhouse, A. R.; Wang, X. H.; Konstantatos, G.; Debnath, R.; Levina, L.; Raabe, I.; Nazeeruddin, M. K.; Gratzel, M.; Sargent, E. H. *ACS Nano* **2010**, *4* (6), 3374–3380.
(10) Clark, S. W.; Harbold, J. M.; Wise, F. W. *J. Phys. Chem. C* **2007**, *111* (20), 7302–7305.
(11) Crooker, S. A.; Hollingsworth, J. A.; Tretiak, S.; Klimov, V. I. *Phys. Rev. Lett.* **2002**, *89* (18), 186802.
(12) Kovalenko, M. V.; Talapin, D. V.; Loi, M. A.; Cordella, F.; Hesser, G.; Bodnarchuk, M. I.; Heiss, W. *Ang. Chem., Int. Ed.* **2008**, *47* (16), 3029–3033.
(13) van Huis, M. A.; Kunneman, L. T.; Overgaag, K.; Xu, Q.; Pandraud, G.; Zandbergen, H. W.; Vanmaekelbergh, D. *Nano Lett.* **2008**, *8* (11), 3959–3963.
(14) Talgorn, E.; Abellon, R. D.; Kooyman, P. J.; Piris, J.; Savenije, T. J.; Goossens, A.; Houtepen, A. J.; Siebbeles, L. D. A. *ACS Nano* **2010**, *4* (3), 1723–1731.
(15) Talgorn, E.; Moysidou, E.; Abellon, R. D.; Savenije, T. J.; Goossens, A.; Houtepen, A. J.; Siebbeles, L. D. A. *J. Phys. Chem. C* **2010**, *114* (8), 3441–3447.
(16) Moreels, I.; Lambert, K.; De Muynck, D.; Vanhaecke, F.; Poelman, D.; Martins, J. C.; Allan, G.; Hens, Z. *Chem. Mater.* **2007**, *19* (25), 6101–6106.
(17) Talgorn, E.; Gao, Y.; Aerts, M.; Kunneman, L. T.; Schins, J. M.; Savenije, T. J.; van Huis, M. A.; van der Zant, H. S. J.; Houtepen, A. J.; Siebbeles, L. D. A. *Nat. Nanotechnol.* **2011**, DOI: 10.1038/nnano.2011.159.
(18) Kocherzhenko, A. A.; Grozema, F. C.; Vyrko, S. A.; Poklonski, N. A.; Siebbeles, L. D. A. *J. Phys. Chem. C* **2010**, *114*, 20424–20430.
(19) Hummel, A., Single-pair diffusion model of radiolysis of hydrocarbon liquids. In *Kinetics of nonhomogeneous processes: a practical introduction for chemists, biologists, physicists, and materials scientists*; Freeman, G. R., Ed.; Wiley-Interscience: New York, 1987; pp 215−304.
(20) Kittel, C. *Introduction to solid state physics*, 7th ed.; John Wiley & Sons: New York, 1996.
(21) Grozema, F. C.; Siebbeles, L. D. A. *Int. Rev. Phys. Chem.* **2008**, *27* (1), 87–138.
(22) Tang, J.; Kemp, K. W.; Hoogland, S.; Jeong, K. S.; Liu, H.; Levina, L.; Furukawa, M.; Wang, X.; Debnath, R.; Cha, D.; Chou, K. W.; Fischer, A.; Amassian, A.; Asbury, J. B.; Sargent, E. H. *Nat. Mater.* **2011**, *10* (10), 765–771.
(23) Lee, J.-S.; Kovalenko, M. V.; Huang, J.; Chung, D. S.; Talapin, D. V. *Nat. Nanotechnol.* **2011**, *6* (6), 348–352.
(24) Klimov, V. I. *Annu. Rev. Phys. Chem.* **2007**, *58*, 635–673.
(25) Schaller, R. D.; Klimov, V. I. *Phys. Rev. Lett.* **2004**, *92* (18), 186601.
(26) Trinh, M. T.; Houtepen, A. J.; Schins, J. M.; Piris, J.; Siebbeles, L. D. A. *Nano Lett.* **2008**, *8* (7), 2112–2117.
(27) Ellingson, R. J.; Beard, M. C.; Johnson, J. C.; Yu, P.; Micic, O. I.; Nozik, A. J.; Shabaev, A.; Efros, A. L. *Nano Lett.* **2005**, *5* (5), 865–871.
(28) Trinh, M. T.; Houtepen, A. J.; Schins, J. M.; Hanrath, T.; Piris, J.; Knulst, W.; Goossens, A. P. L. M.; Siebbeles, L. D. A. *Nano Lett.* **2008**, *8* (6), 1713–1718.
(29) Talgorn, E. C. V.; Gao, Y.; Aerts, M.; Kunneman, L. T.; Schins, J. M.; Savenije, T. J.; van Huis, M. A.; Van der Zant, H. S. J.; Houtepen, A. J.; Siebbeles, L. D. A. *Nat. Nanotechnol.*, in press.
(30) Aerts, M.; Suchand Sandeep, C. S.; Gao, Y.; Savenije, T. J.; Schins, J. M.; Houtepen, A. J.; Kinge, S.; Siebbeles, L. D. A. *Nano Lett.* **2011**, *11* (10), 4485–4489.
(31) Schaller, R. D.; Pietryga, J. M.; Goupalov, S. V.; Petruska, M. A.; Ivanov, S. A.; Klimov, V. I. *Phys. Rev. Lett.* **2005**, *95* (19), 196401.
(32) Bockelmann, U.; Bastard, G. *Phys. Rev. B* **1990**, *42* (14), 8947.
(33) Benisty, H.; Sotomayor-Torres, C. M.; Weisbuch, C. *Phys. Rev. B* **1991**, *44* (19), 10945.
(34) Klimov, V. I.; McBranch, D. W. *Phys. Rev. Lett.* **1998**, *80* (18), 4028–4031.
(35) Wehrenberg, B. L.; Wang, C. J.; Guyot-Sionnest, P. *J. Phys. Chem. B* **2002**, *106* (41), 10634–10640.
(36) Pandey, A.; Guyot-Sionnest, P. *J. Phys. Chem. Lett.* **2010**, *1* (1), 45–47.
(37) Pandey, A.; Guyot-Sionnest, P. *Science* **2008**, *322* (5903), 929–932.
(38) Guyot-Sionnest, P.; Wehrenberg, B.; Yu, D. *J. Chem. Phys.* **2005**, *123* (7), 074709.
(39) Nozik, A. J. *Phys. E (Amsterdam, Neth.)* **2002**, *14* (1−2), 115–120.
(40) Tisdale, W. A.; Williams, K. J.; Timp, B. A.; Norris, D. J.; Aydil, E. S.; Zhu, X. Y. *Science* **2010**, *328*, 1543–1547.